International Journal of Research in Engineering and Science (IJRES)
ISSN (Online): 2320-9364, ISSN (Print): 2320-9356
www.ijres.org Volume 9 Issue 8 ǁ 2021 ǁ PP. 01-13

Recycling post-consumer polypropylene as Fuel: Kinetics study of the combustion of post-consumer food container made of poly(propylene)

Nasrollah Hamidi[1], Allisanne Sarvis[2]
South Carolina State University, Orangeburg, SC 29117 USA
1. Corresponding author
2. Undergraduate student

Abstract
In modern society, daily food is packaged in various kinds of plastics including polypropylene (PP) which after consumption disposed of as wastes. These disposals have a yearly growth rate of over 5%; therefore they are available as a pseudo renewable resource for a variety of uses. Occasionally, waste plastics (WP) have been used to produce energy. Here we studied the kinetics of combustion of post-consumer samples of a thin-walled food container made of pp (PC-PP) by thermogravimetric analysis (TGA) under a stream of breathing air to determine its thermal-oxidative kinetics parameters by the isoconversional method using five heating rates, β = 1, 5, 10, 25, and 50 K/min. The values of initial decomposition temperature, the temperature at the maximum combustion rate, and the maximum rate of decomposition were increased by increasing the heating rates, as was expected. The values of activation energy barrier $\boldsymbol{E_a}$ (kJ/mol) was relatively constant at the extents of reaction, $\alpha < 0.65$; but at higher α values the $\boldsymbol{E_a}$ values increased as the value of α increased, independent of the $f(\alpha)$, the model used. The PC-PP combustion mechanism at $\alpha < 0.85$, which had a low energy barrier could predominantly occur via the polymer-peroxide pathway. However, at $\alpha > 0.85$ the energy barrier of combustion was very high close to the bond energy of the chain scissoring mechanism.

Keywords: *recycling; upcycling; combustion; polyethylene, mechanism; waste plastics; post-consumer poly(propylene) (PC-PET); pyrolysis; isoconversional method; thermoxidative degradation; activation energy;wast polypropylene; incerenation.*

Date of Submission: 23-07-2021 Date of acceptance: 08-08-2021

I. Introduction

Polypropylene (PP) has superior barrier properties, high tensile strength, and desirable surface finish, optical clarity, low moisture/vapor transmission, low cost and easily is blow-molded for manufacturing. It is the source of many commodities such as bottles, crates, pots, films, graphic arts applications, disposable diaper tabs, numerous packaging applications utilities, and thin-walled containers and bags that are usually used for food packaging. The global production of polypropylene resin was 56.0 Million Metric Tons (MMT) in 2018 and is projected to reach around 88.0 MMT by 2026, growing at a rate of approximately 5.7% per year. The production of PP resin in the USA was 7.7 MMT in the same year.[1,2] Principal use of PP is in the packaging industry in the forecasted period.[3] The other consumer of PP is the automotive industry for producing lightweight, affordable, and fuel-efficient vehicles. Thus, it is important to understand the thermal stability and thermal-oxidative properties of disposed PP (PC-PP) as a part of recycling, reusing, and incinerating wastes. Occasionally, PC-PP is used as fuel to recover its internal energy. In this work, we study its thermo-oxidation behavior under a birthing air atmosphere. The kinetics of combustion of PC-PP is important in the context of thermochemical conversion processes aimed at the use of PC-PPs as a source of energy (fuel) under a breathing air atmosphere.[4,5]

Thermal degradation of polymers and the degradation kinetics under inert and oxidative atmospheres by thermogravimetric analysis (TGA) have been at the center of thermal analysis studies for many years. [e.g. 6,7,8] By using proper methods for kinetic evaluations, the kinetic analysis may effectively assist in exploratory combustion mechanisms as well as in predicting the adequated environment for its combustion.[9,10] Thermal oxidation of PP similar to other polymeric materials involves chemical complexity and a large number of different reactions.[e.g.,6-20] The apparent mass loss kinetic models developed so far fall into two categories: (i) pseudo-single-component overall models (PSOM) [11,12] and (ii) pseudo-multi-component overall models (PMOM). [13,14] In this study the PSOM model was used since it has been used successfully to describe the thermolysis of PP [6] and other synthetic polymers [15] such as poly(ethylene terephthalate) [16,17], and natural

polymers such as cellulose [18], lignin [19,20], hemicellulose [21], xylan [22] and the biomass decomposition [18,23]

The major practical purpose of this work is the prediction of process rates and material lifetimes of the PC-PP when it has been used as fuel in air atmosphere incinerators and high-temperature reactors. The predictions and kinetic analysis are based on reliable isoconversional method with the theoretical purpose of the interpretation of experimentally determined, fundamental, theoretical concepts associated with the kinetics of PC-PP, known as the kinetics triplets; in our case, the activation energy barrier, $\mathbf{E_a}$, the frequency of vibrations of the activated complex, **A,** and the reaction mechanism expressed in the form of the α-functions, $f(\alpha)$, as defined within the text below and tabulated in **Table 1**.

Table 1. *The kinetic models that have been used in this work.*

No.	Reaction Model	Code	$f(\alpha)$
1	Power law	P4	$4\alpha^{3/4}$
2	Power law	P3	$3\alpha^{2/3}$
3	Power law	P2	$2\alpha^{1/2}$
4	Power law	P2/3	$2/3\alpha^{-1/2}$
5	One-dimensional diffusion	D1	$1/2\alpha^{-1}$
6	Mampel (first order)	F1	$(1-\alpha)$
7	Avrami–Erofeev	A4	$4(1-\alpha)[-\ln(1-\alpha)]^{3/4}$
8	Avrami–Erofeev	A3	$3(1-\alpha)[-\ln(1-\alpha)]^{2/3}$
9	Avrami–Erofeev	A2	$2(1-\alpha)[-\ln(1-\alpha)]^{1/2}$
10	Three-dimensional diffusion	D3	$3/2(1-\alpha)^{2/3}[1-(1-\alpha)^{1/3}]^{-1}$
11	Contracting sphere	R3	$3(1-\alpha)^{2/3}$
12	Contracting cylinder	R2	$2(1-\alpha)^{1/2}$
13	Two-dimensional diffusion	D2	$[-\ln(1-\alpha)]^{-1}$
14	Random Scission	L2	$2(\alpha^{1/2}-\alpha)$

Aiming to find an accurate kinetic method suitable for PC-PP oxidation in an atmosphere similar to those that reuse PC-PP as fuel, five temperature scans of five PC-PP samples, instead of a single one, were used to improve both the discrimination of the reaction mechanism and the determination of the kinetic parameters; since it is unreliable to estimate the kinetic parameters [24] and kinetic model simultaneously from the same experiment.[25,26]

II. Experimental

The PC-PP samples were obtained from a post-consumer, 16 oz thin-walled food container from an unknown provider without further treatments. 12 circular samples of 4 mm diameter, a size suitable to fit in a TGA pan were cut from its sidewall. One flat piece of PC-PP was loaded into the TGA sample pan with the initial masses of ~ 4-6 mg (**Table 2**, column 1). The depth of the sample layer filled in the pan was equal to the thickness of the container, less than 1 mm and well below the top of the pan. Thermal decomposition of combustion was observed in terms of the overall mass loss by using a TGA-7 Thermogravimetric Analyzer (PerkinElmer, Inc., USA). Temperature calibration of the TGA was carried out with special concern since the thermocouple in this device was not in direct contact with the sample. The airstream was continuously passed into the furnace at a flow rate of 80 mL/min at room temperature and atmospheric pressure. The temperature program was held at 50 °C for 1 min, and subsequently increased to 850 °C at the rates (β) of 1, 5, 10, 25, and 50 K/min and held at the 850 °C for 3 min. The sample mass loss percentages and their temperatures were recorded continuously as a function of heating time. The data was downloaded and converted to Microsoft Excel format for further analysis.

The extent of conversion, α, which is the fraction of reacted materials was determined experimentally as a fraction of the weight-loss as:

$$\alpha = (m_i - m)/(m_i - m_f)$$

where m_i is the original sample mass, m is the sample mass at a given temperature, and m_f is the mass of the sample at the end of the reaction which was estimated by the onset at the end of the thermogram. The values of α increased from zero to one as the thermal degradation progressed from initiation to completion. The value of α typically reflects the progress of the overall transformation of PC-PP reactants to products, since the physical properties measured by the thermal analysis methods are not species-specific and, thus, cannot be linked directly to a specific reaction of thermoxidative degradation processes of the PC-PP molecules.

III. Kinetic Theory

The thermally stimulated decomposition of PC-PP took place at temperatures over 200 °C, above the melting point (mp) of PP (~ 130-175 °C) [27] in its liquid phase. The kinetics of the thermal decomposition of PC-PP, which deals with the measurement and parameterization of the process rates, can be expressed by Eq.1:

$$\text{(Eq. 1)} \qquad \textit{PC-PP (solid)} \xrightarrow{\Delta} \textit{PC-PP (liquid)} \xrightarrow{\Delta} \textit{A (solid or liquid) + B (gas)}$$

The reverse reaction is not energetically favorable and was prevented by a well-controlled 80 mL/min. airstream, which reacted with the PC-PP and carried the volatiles away as soon as they formed. The thermally stimulated processes of the decomposition of PC-PP and other polymers under constant pressure are parameterized in terms of major variables such as a temperature-dependent rate constant [k(T)], and the extent of conversion (α), where (1-α) represents the residual amount of reactant: [28, 29, 30]

(Eq. 2) $$\frac{d(1-\alpha)}{dt} = -k(T)f(\alpha)$$

The overall transformation, at high temperatures, can involve many simultaneous single and/or, multi-step reactions, each of which has its specific α and k, where the kinetics of the reactions has been dominated by the slowest one, expressed by Eq. 3.

(Eq. 3) $$\frac{d(\alpha)}{dt} = k(T)f(\alpha)$$

The temperature changed linearly with time, with the constant heating rate, β, being controlled by the TGA-7 instruments in agreement with the program settings. The most common kinetic functions that describe the mechanisms of a reaction expressed in the function of $f(\alpha)$ [31], which are published widely by many authors and are presented in **Table 1**. The reaction models are of three major types: accelerating (A), decelerating (D) and sigmoidal (σ) or autocatalytic, as shown in Fig. 1**a**. [32-32] The PC-PP experimental model profiles displayed in Fig. 1**b** show a series of similar curves, displaced from one another on the time axis, similar to the sigmoidal one[33].

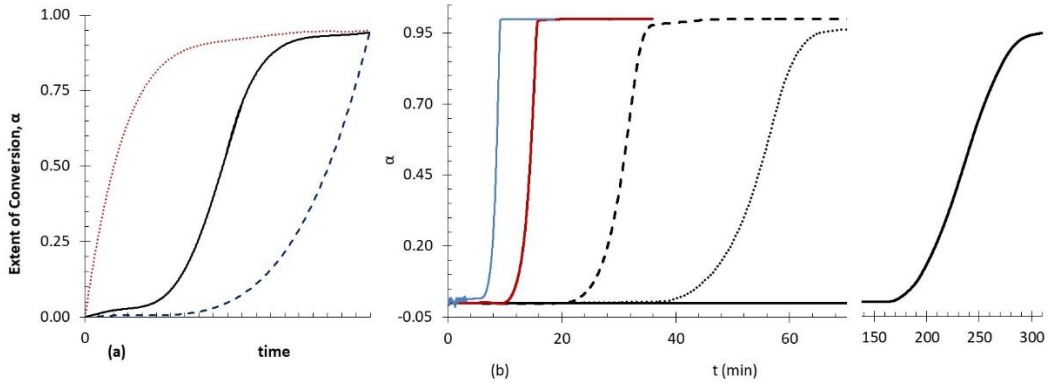

Fig. 1**. *(a)***. Theoretical reaction profiles models: (A) accelerating, (D) decelerating, and (σ) sigmoidal. **(b)** The experimental thermo-oxidative reaction profiles of PC-PP for the β (K/min) = 1, 5, 10, 25 and 50, from right to left, respectively.

Let us assume that all processes have an Arrhenius temperature dependence express as Eq. (4).

(Eq. 4) $$k(T) = A\ Exp\left(-\frac{E_a}{RT}\right)$$

where **A** is the pre-exponential factor of Arrhenius, $\mathbf{E_a}$ is the activation energy of the reaction, R = 8.314 J mol^{-1} K^{-1} is the universal gas constant and T is the absolute temperature. The experimental kinetic parameters obtained by this assumption are called "effective", "apparent", "empirical", or "global" since they are different from intrinsic parameters. Combining Eqs. (3) and (4) yield:

(Eq. 5) $$\frac{d\alpha}{dt} \equiv k(T)f(\alpha) = f(\alpha)\ A\ Exp\left(-\frac{E_a}{RT}\right)$$

The above relationships were developed for gaseous reactions and have been applied successfully to the thermal degradation of polymers. Eq. 5 is the basis for various differential kinetic methods. It applies to any temperature program, be it isothermal or non-isothermal. According to Eq. 6, the slope of a plot of ln[(dα/dt)/ $f(\alpha)$] = ln k versus 1/T, known as the Arrhenius plot, yields the value of (-$\mathbf{E_a}$/R), independent of the $f(\alpha)$ model used and the intercept is the value of ln**A**.

(Eq. 6) $$ln\left[\frac{\left(\frac{d\alpha}{dt}\right)}{f(\alpha)}\right] = ln\ k = -\frac{E_a}{RT} + lnA$$

IV. Results And Discussion

4.1. Characteristics of the mass loss curves

Figure 2(a) shows the five normalized PC-PP samples' weight-loss percentages versus the sample temperature at varying heating rates (β) of 1, 5, 10, 25, and 50 K/min under a breathing air atmosphere. The weight loss of PC-PP under an inert nitrogen atmosphere at β =25 K/min. was included for comparison. The rates of weight loss (-dα/dt) obtained from the negative derivatives of TGA curves with time are represented in **Fig. 2(b).**

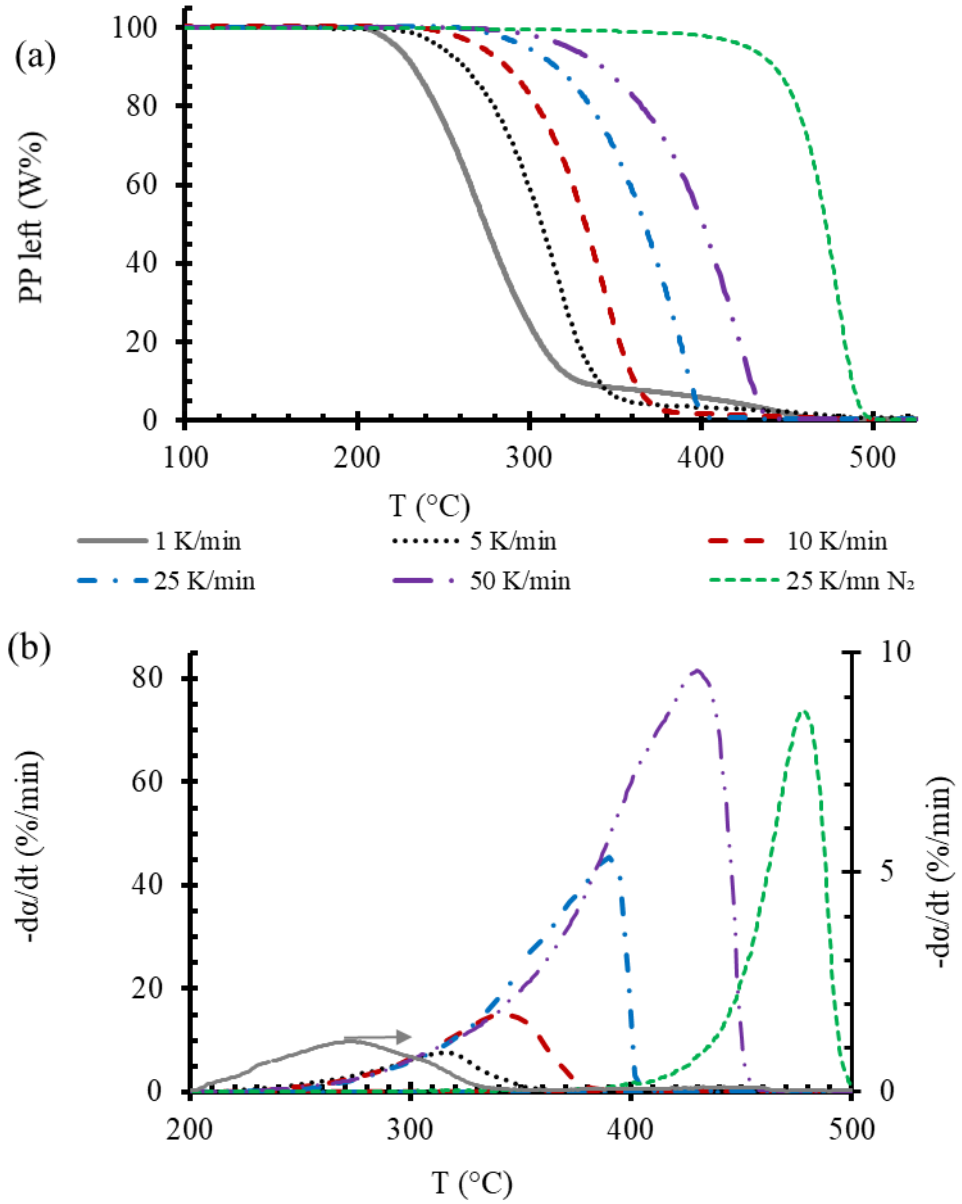

Fig. 2**.** Experimental TGA and rate of decomposition curves for the oxidative degradation of PC-PP. **(a)** Normalized weight loss at ß = 1, 5, 10, 25, and 50 K/min, from left to right, respectively, and PC-PP degradation under a nitrogen atmosphere at 25 K/min. **(b)** Combustion rate for the same samples.

Figures 2a and **2b** show individual curves, similar in shape, that are displaced one from the other along the temperature axis; which may suggest that a similar order of reaction carried over the heating rate range. In nitrogen and air at $\beta \geq 10$ K/min, PC-PP degrades in a single step, however, in the presence of air at the $\beta \leq 5$ K/min, there also appears to be an additional small step that occurs in the w% < 8 %, at the end of the decomposition reaction, similar to the decomposition of polystyrene (PS) in air as reported by other researchers.[6]

Some characteristic quantities of thermal stability such as the initial decomposition temperature (T_i), the half-weight loss temperature ($T_{50\%}$), the final decomposition temperature (T_f)[34,35], the maximum decomposition rate (R_{max}), the extent of reaction and temperature corresponding to R_{max} (α_{max}, T_{max}, respectively), [36] have been evaluated and tabulated in **Table 2.** The same values for degradation of PC-PP under nitrogen environment are listed in the last row in **Table 2**.

Table 2. Features of the thermograms of PC-PP samples in an air and nitrogen atmosphere (T are in °C)

Sample	M_{sample}	ß	$T_{98\%}$	$T_{90\%}$	$T_{50\%}$	$T_{20\%}$	T_f	W_f%	R_{max}	T_{max}	α_{max}	under
1	5.658	1	214	233	275	306	341	8.8	1.26	275	0.54	Air
2	4.338	5	236	262	307	328	388	3.7	7.7	316	0.63	Air
3	4.682	10	257	287	333	352	383	2.2	15.1	343	0.65	Air
4	5.013	25	282	316	367	388	409	0.7	45.6	390	0.84	Air
5	5.902	50	303	342	401	423	431	6.7	81.5	422	0.80	Air
PC-PP/N_2	5.608	25	399	443	472	484	530	0.2	74.0	478	0.69	N_2

The results in **Table 2** show that these qualitative criteria of polymer stability obtained from the TGA curves increase regularly with increasing heating rate, which may result in different characteristic temperatures being reported in other β values, as expected.

The maximum rate of combustion increased with the values of β. The shape of the rate curve at β = 1 K/mol is nearly symmetric and centered at α = 0.54. However, for other values of β > 5 K/mol, the values of R_{max} fall within the values of α > 0.5 range, as shown in **Table 2**, 10th column.

4.2. Estimation of Kinetics Parameters by Isoconversional Methods

The use of isoconversional methods and the data obtained from five heating rates help to obtain reliable values of $\mathbf{E_a}$ of thermo-oxidative degradation of PC-PP and other related kinetic parameters at each extent of reaction. **Figure 3** shows the model-free-fitting of the experimental data obtained from multiple heating rates of PC-PP under a breathing air atmosphere according to the isoconversional method, **Eq.** 6. [37] In theory, this method delivers activation energies similar to the values obtained by the isothermal methods at any α value, according to many authors. [e.g. 36,38] **Figure 4(A)** shows the variation of $\mathbf{E_a}$ for the oxidation of PC-PP versus the extent of reaction, α. **Table 3** shows the values of $\mathbf{E_a}$ obtained for the 14 extents of reaction covering a wide range of **α** values, 0.05 < **α** < 0.95, and corresponding to heating rates ranging from 1 to 50 K/min which their corresponding $\mathbf{r^2}$ values are shown in **Fig. 5**. The corresponding values of ln**A** obtained from the intercept of the lines in **Fig. 3** are tabulated in **Table 4** and were visualized in **Fig. 4(B).**

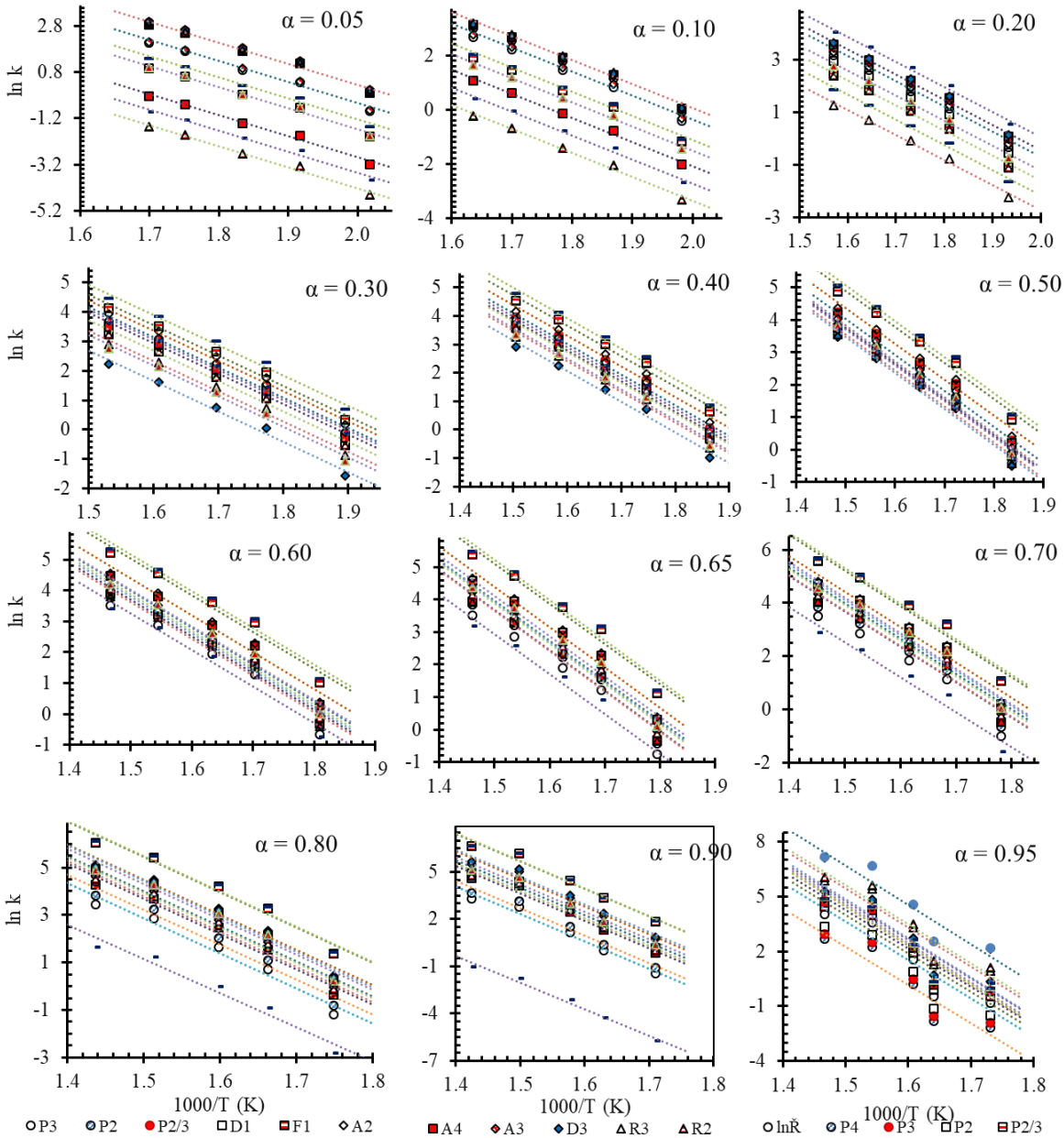

Fig. 3. Isoconversional estimations of $\mathbf{E_a}$ for the oxidation of PC-PP under variable heating rates and a breathing air atmosphere.

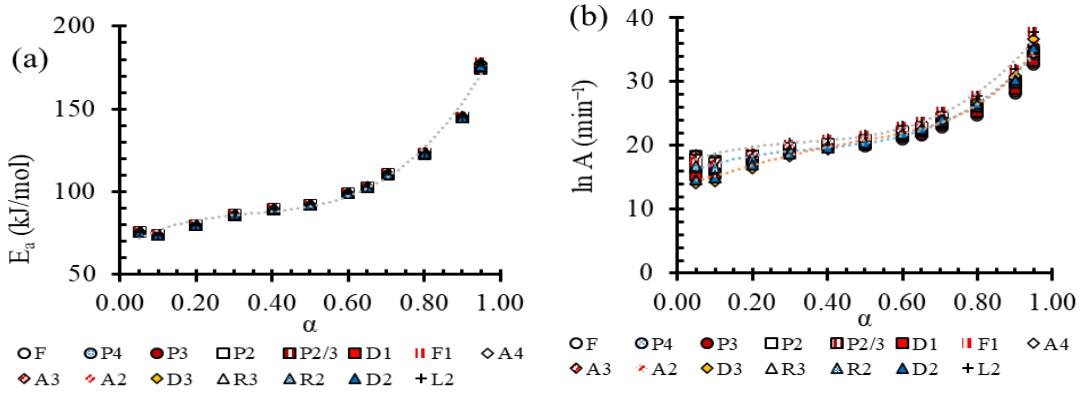

Fig. 4. Variations of PC-PP thermal oxidation parameters with the extent of reaction. (a) Variation of $\mathbf{E_a}$ versus **α**, and (b) variation of ln**A** versus **α**

The values of $\mathbf{E_a}$ obtained from the slopes of the adjusted lines in **Fig. 3** are listed in **Table 3** were near to each other, independent of the $f(\alpha)$ function used in **Eq. 6** for a given $\boldsymbol{\alpha}$ value. For example, the average $\mathbf{E_a}$ obtained from the slope of all models at $\boldsymbol{\alpha}$ = 0.50 was $\mathbf{E_a}$ = 92.2±0.1 kJ/mol, and the corresponding intercepts were ln**A** =21.5 ± 0.4. Comparison fo **Fig. 4(a) and (b)** shows the values of ln**A** are more scattered than the values of $\mathbf{E_a}$. Since the values of $\mathbf{E_a}$ obtained by model-free isoconversional methods are not associated with reaction model-fitting [9]; but the intercept of the model caries the effects of $f(\alpha)$ as shown by **Eq.** 6. However, these kinetic parameters of the thermo-oxidative degradation of PC-PP can provide practical, important information on how it behaves under more realistic atmospheric conditions.

The trends of variation of the values of $\mathbf{E_a}$ versus α obtained in this work for the degradation of PC-PP (74-176 kJ/mol) is very similar to the variations reported by Peterson et al (80 to 220)[6], however, our values were slightly smaller; due to differences on the nature of materials being used and the computational effects as reported by other researchers [6,39,40,41] Frequently, the reliability of the estimated Arrhenius parameters by fitting kinetic data to a reaction model is subject to the proper choice of the reaction model. As the application of the model-fitting procedure to a single heating rate curve gives rise to a value of $\mathbf{E_a}$ that may differ over an order of magnitude by simply choosing a different reaction model;[41] though they show similar correlation coefficients. In this work, model-free isoconversional methods are used to overcome the problems associated with model-fitting as shown in **Fig. 4**.

Analysis of the dependence of the values of $\mathbf{E_a}$ and ln **A** to $\boldsymbol{\alpha}$ as shown by **Figs. 4 A & B** provides important clues about changes in the reaction mechanism. Some kinetic factors such as the surface area of a reacting sample do not directly affect the activation energy, but the effective value of **A**. Trustworthy estimation of the values of **A** and hence thermodynamics functions may in principle provide additional mechanistic clues. However, the obtained values of **A** tend to be strongly correlated with the values of $\mathbf{E_a}$ via compensation effect, which makes the **A** factor to be dependent on $\mathbf{E_a}$, as was observed by comparison of the data in **Figs. 4(a) & 4(b)**.

In the case of PC-PP, for all values of $\boldsymbol{\alpha}$ and all models presented in **Table 1**, the variation of lnk versus 1/T yielded a straight line with a similar slope ($\mathbf{E_a}$/R) for a given value of α as shown in **Fig. 3,** and **Table 3**. Though the appropriate model must be a sigmoidal one, all models were adjusted to the isoconversional thermal degradation data. **Figure 5** compares the variation of the values of $\mathbf{r^2}$ for all models at each $\boldsymbol{\alpha}$; according to the numbers assigned to the models in **Table 1**.

The expectation was that the higher values of $\mathbf{r}^2$ would be for models 7, 8 and 9 as observed for $\boldsymbol{\alpha}$ = 0.10, 0.20, and 0.95. However, according to the comparisons of $\mathbf{r^2}$ values in **Fig. 5,** the highest $\mathbf{r}^2$ values were observed for the kinetic model 10 corresponding to three-dimensional diffusions. Power law 1, 2, and 3 also were within acceptable models for α = 0.1, 0.20 and 0.95. The best fitting of the different reaction models to the different extents of reactions could be an indication of the dependence of the degradation mechanism on the extent of the reaction. This could be justified by considering at each extent of the reaction, the composition of reactants was changed since the original PC-PP under high temperatures was converted to non-volatile sub-chains and longer chains with conjugated systems, in the thermal oxidation process. In this manner, the materials under the study at the various extent of reaction were different from each other and so too would be the mechanism of the reaction.

The effective activation energies estimated for PC-PP, listed in **Table 3,** are most likely to be a composite value determined by the sum of activation energy barriers of the involved individual steps. The effective activation energy can vary strongly with the temperature and the extent of conversion [41] as was observed in **Fig. 4(a)**. Such discrepancies are not typically expected for the activation energy barrier of a simple elementary individual type of chemical reaction.

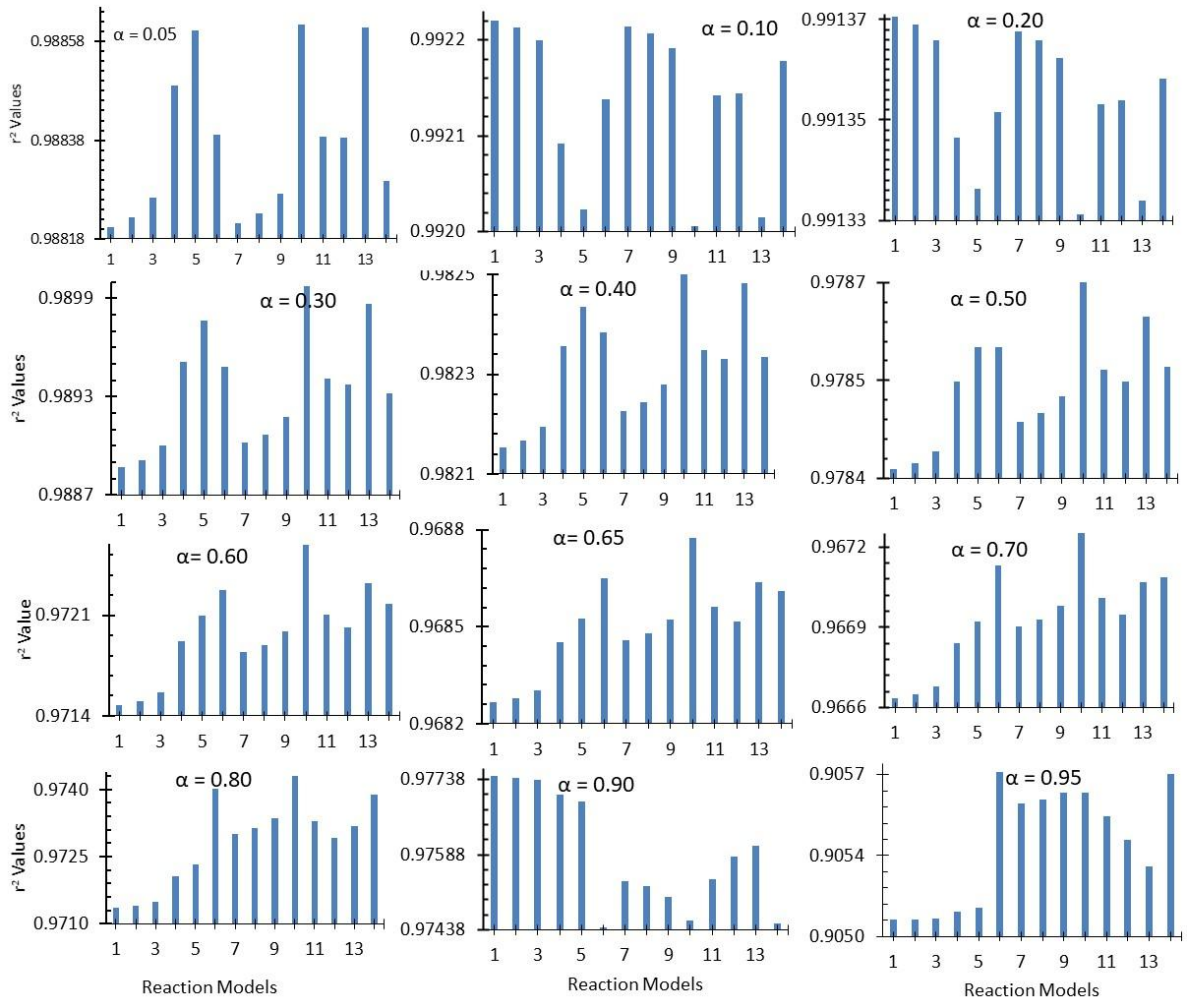

Fig. 5. *Representation of* r^2 *values of* ***Eq. (8)****, lnk versus 1/T (K), of the 14 f(α) tabulated in* ***Table 1.***

Table 3. The $\mathbf{E_a}$ values for the corresponding **α** values are evaluated from the related *f*(α) function of the models in **Table 1**.

α	F	P4	P3	P2	P2/3	D1	F1	A4	A3	A2	D3	R3	R2	D2	L2	Average	STDVE
0.05	75.6	75.5	75.5	75.6	75.7	75.7	75.6	75.5	75.5	75.6	75.7	75.6	75.6	75.7	75.6	75.6	0.1
0.10	73.8	73.8	73.8	73.8	73.8	73.8	73.8	73.8	73.8	73.8	73.8	73.8	73.8	73.8	73.8	73.8	0.0
0.20	79.7	79.6	79.7	79.7	79.7	79.7	79.7	79.7	79.7	79.7	79.7	79.7	79.7	79.7	79.7	79.7	0.0
0.3	85.8	85.6	85.6	85.7	86.0	86.2	86.0	85.7	85.7	85.8	86.3	85.9	85.9	86.3	85.9	85.9	0.2
0.40	89.4	89.4	89.4	89.4	89.5	89.5	89.5	89.4	89.4	89.4	89.6	89.5	89.5	89.5	89.5	89.5	0.1
0.50	92.1	92.0	92.0	92.0	92.1	92.2	92.2	92.1	92.1	92.1	92.4	92.2	92.2	92.3	92.2	92.1	0.1
0.60	99.1	99.0	99.0	99.0	99.1	99.2	99.3	99.1	99.1	99.2	99.4	99.2	99.2	99.3	99.2	99.2	0.1
0.65	102.7	102.7	102.7	102.7	102.8	102.8	102.9	102.8	102.8	102.8	103.0	102.9	102.8	102.9	102.9	102.8	0.1
0.71	110.6	110.4	110.4	110.5	110.6	110.7	110.9	110.7	110.7	110.8	111.1	110.8	110.7	110.9	110.9	110.7	0.2
0.80	122.8	122.6	122.7	122.7	122.9	123.1	123.8	123.4	123.4	123.5	123.9	123.5	123.3	123.4	123.8	123.3	0.4
0.90	144.8	144.7	144.7	144.8	144.8	144.9	145.6	145.3	145.3	145.4	145.5	145.3	145.2	145.1	145.5	145.2	0.3
0.95	174.4	174.3	174.3	174.3	174.5	174.6	178.5	177.5	177.6	177.8	177.9	177.2	176.5	175.8	178.5	176.4	1.7

Table 4. *The value of ln**A** for each **α** corresponding to the respective models indicated in* ***Table 1.***

α	F	P4	P3	P2	P2/3	D1	F1	A4	A3	A2	D3	R3	R2	D2		Average	STDVE
0.05	17.6	18.4	18.5	18.4	16.5	15.3	17.7	18.5	18.5	18.4	14.0	16.5	16.9	14.7	18.6	17.1	1.6
0.10	17.3	17.6	17.7	17.7	16.5	15.7	17.4	17.7	17.8	17.8	14.4	16.2	16.6	15.0	18.1	16.8	1.2
0.20	18.5	18.3	18.5	18.6	18.1	17.6	18.7	18.5	18.6	18.8	16.4	17.6	17.9	17.0	19.2	18.0	0.7
0.30	19.7	19.2	19.4	19.6	19.6	19.3	20.1	19.4	19.6	19.9	18.3	18.9	19.2	18.8	20.4	19.3	0.5
0.40	20.4	19.7	19.9	20.1	20.3	20.2	20.9	20.0	20.2	20.5	19.3	19.6	19.9	19.7	21.1	20.0	0.4
0.50	20.8	19.9	20.1	20.4	20.9	20.8	21.5	20.4	20.6	21.0	20.1	20.2	20.5	20.5	21.7	20.5	0.4
0.60	22.0	21.0	21.2	21.5	22.2	22.2	22.9	21.6	21.9	22.3	21.7	21.5	21.8	21.9	23.1	21.8	0.5
0.65	22.6	21.5	21.8	22.1	22.8	22.9	23.7	22.2	22.5	23.0	22.5	22.2	22.4	22.7	23.8	22.5	0.6
0.71	24.0	22.8	23.1	23.4	24.2	24.3	25.2	23.7	24.0	24.4	24.2	23.7	23.9	24.2	25.3	23.9	0.6
0.80	26.0	24.7	25.0	25.4	26.3	26.5	27.8	25.9	26.3	26.8	26.8	26.1	26.2	26.6	27.8	26.2	0.8
0.90	29.5	28.2	28.4	28.8	29.8	30.1	31.9	29.9	30.2	30.8	30.9	30.0	30.0	30.4	32.0	30.0	1.0
0.95	34.0	32.6	32.9	33.3	34.4	34.7	37.8	35.4	35.8	36.4	36.7	35.5	35.2	35.4	37.8	35.1	1.5

Mechanism of the reaction

In TGA experiments, the initiation step is induced by temperature. Although, other physical effects such as radiation, mechanical treatment, and some chemical factors such as the traces of peroxide initiators and hydro-peroxides are also known to initiate a reaction.[42]

The energy barrier to the reaction of the molecular oxygen with the C–H bonds in any organic molecule is very high. This makes the combustion and oxidation mechanisms multifaceted, with a multitude of possible steps following initiation, which typically occur by the formation or introduction of a radical.[43] Subsequently, chain propagation steps follow, and many different types of radicals can play a role. Because of this, most oxygen-initiated oxidation has activation energies in the range of 80–110 kJ/mol. Oxygen molecules in their ground state possess a di-radical configuration (· O=O·), but it is not able to initiate the reaction. The formation of an oxygen di-radical as a peroxy, · O-O· requires $E_a = (E_{O=O} - E_{\cdot O\text{-}O\cdot} = 498\text{-}146 =)$ 352 kJ/mol, and the formation of a set of two carbon radical by cleaving methyl group from the PP chain requires E_a = 355 kJ/mol, and the cleavage of the tertiary hydrogen of PP require 385 kJ/mol as shown in **Fig. 6.**

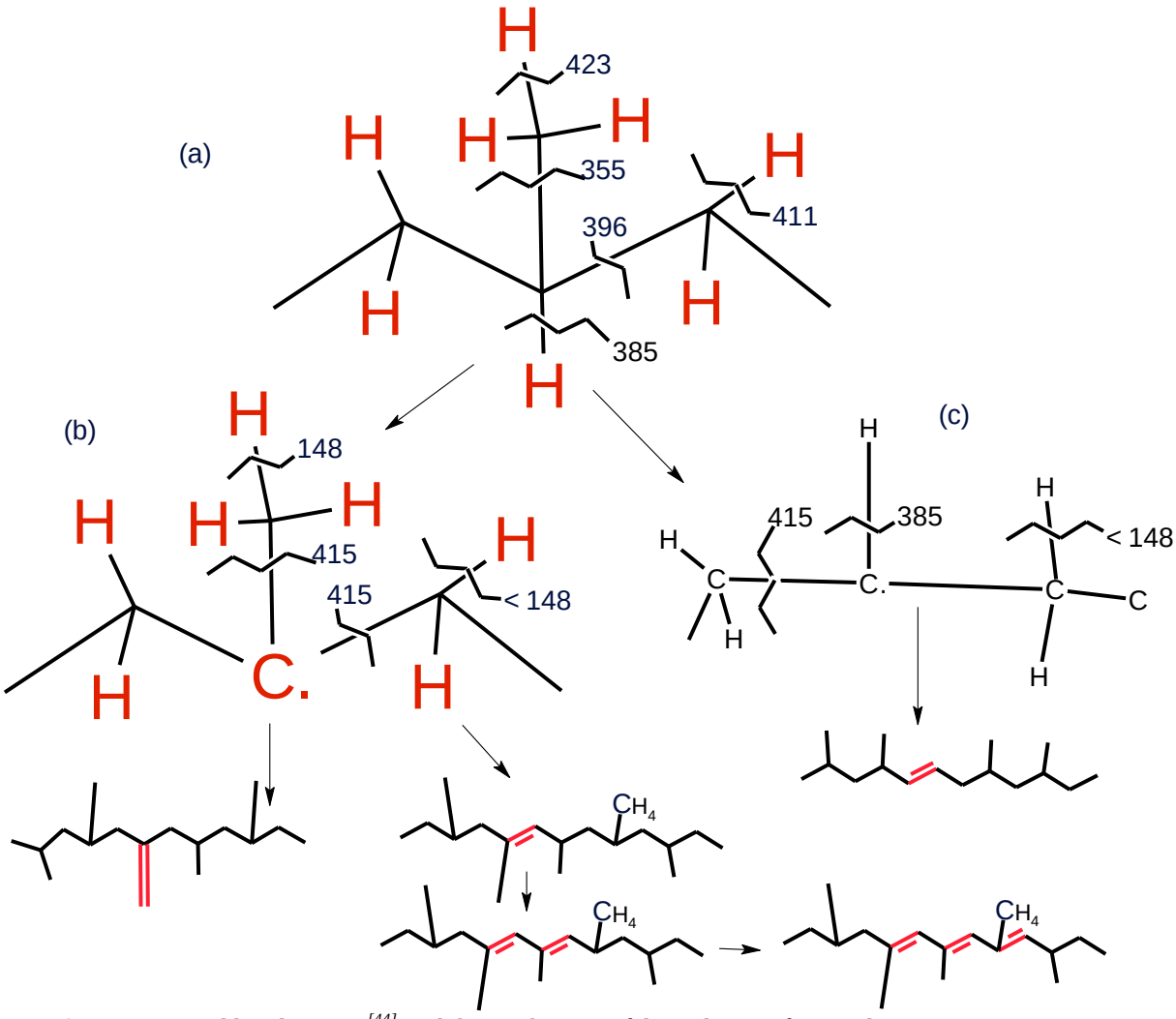

Fig. 6. *Estimated bond energy [44] and the mechanism of degradation of PP under an inert environment.*

Most likely, the hydrogen abstraction step in autoxidation reactions involves peroxyl radicals, R-O-O· or · O-O· , not the much more plentiful · O=O· diradicals [43]. The · O=O· participate in the radical coupling in the second chain-propagating step. It is known that the thermo-oxidation of most vinyl polymers at moderate temperatures are very similar; they initiate by a peroxy-radical formation and propagate by the hydro-peroxides. The following are some possible steps and their energy barrier:

R-O-O-Ŕ → R-O· + Ŕ -O·	ΔH° = 196 kJ/mol	(a1)
R-O-O –H → R-O-O. + H.	ΔH° = 355 kJ/mol	(a2)
· O=O· → · O-O·	ΔH° = 352 kJ/mol	(a3)
PP-H + · O-O· →PP· + · O-O-H	ΔH° = 404-355 = 48 kJ/mol	(a4)
PP-H → PP· + H·	ΔH° = 385 kJ/mol	(a5)
$PP\text{-}CH_3$ → PP· + · CH_3	ΔH° = 355 kJ/mol	(a6)

Hydrogen atom abstraction by · O-O-H is ~ 160 kJ/mol more favorable, enthalpically than hydrogen atom abstraction by · O=O· . Therefore, the peroxy radical, HOO, would abstract hydrogen of PP−H in the first chain initiation reaction of an autoxidation process. But · O=O as a triplet di-radical would not involve in abstracting hydrogen from PP−H, even when it is present in a very large excess.[43] The decomposition of PC-PP in the absence of peroxides and oxygen initiated at temperature ~ 399 °C under a nitrogen atmosphere but the same reaction starts at temperatures ~ 282 °C under the oxygen, breathing air atmosphere (**Fig. *2***). This is an indication that the initiator in the thermal oxidation of PC-PP reactions was not the same as was in the nitrogen atmosphere, and the peroxide impurities were not initiating the decomposition reactions. Therefore a given form of oxygen with a very low $\mathbf{E_a}$ reaction such as peroxy-di-radical-oxygen (· O-O· (reaction a4)) could initiate the reaction; but not the self-radicalization of PP which have higher $\mathbf{E_a}$ such as the reactions (a5), and (a6).

Consequently, the most probable initiator is peroxy-di-radical oxygen, ˙ O-O˙ , in absence of any peroxide and other impurities. The initiation process is an endothermic one with a barrier of $\mathbf{E_a}$ ~ 75 kJ/mol (**Table 3** first row). In a radical mechanism, the tertiary hydrogen in the C-H backbone is the most active hydrogen, which could be radicalized by peroxy-di-radical oxygen to give a stable tertiary carbon radical as shown in reaction (i).

$[\ldots(\text{-HC}(CH_3)CH_2)_n\text{-}\ldots] + \text{.O-O.} \rightarrow [\ldots(\text{-.C}(CH_3)CH_2)\ (HC(CH_3)CH_2)_{n-1}\text{-}\ldots]\dot{} + \text{H-O-O}\dot{}$ (i)
Or in general: PP-H + .O-O. → PP˙ +˙ O-O-H
$\Delta H = H_{C-H} - H_{H-O-O} = 404 - 355 = +48$ kJ/mol, endothermic

Once the tertiary carbon radical is formed, the activities of α-hydrogens to the carbon radical increase with a substantial decrease on their energy barrier (from over 411 to ~148 kJ/mol) as shown in schemes (b) and (c) of **Fig. 6**. At propagation steps, the abstraction of α-Hs by triplet di-radial oxygen becomes more favorable. Perhaps this causes the lowering energy barrier at α ~ 0.10. Thermo- oxidation reactions propagate via a combination of oxygen molecules with the newly formed PP-radical to form a peroxy radical intermediator, which is a di-radical combination with a very low energy barrier as shown in the reaction (ii)

$[\ldots(\text{-}\dot{} C(CH_3)CH_2)(HC(CH_3)CH_2)_{n-1}\text{-}\ldots] + \dot{} O{=}O\dot{} \rightarrow [\ldots\text{-}(\dot{} O\text{-}O\text{-}C(CH_3)CH_2)(HC(CH_3)CH_2)_{n-1}\text{-}\ldots]$ (ii)
Or simply $PP\dot{} + O_2 \rightarrow PP\text{-}O\text{-}O\dot{}$ $\Delta E = 495 - 358 - 143 = -6$ kJ/mol, exothermic

Reaction (ii) has low activation energy, so it does not affect the rate of reaction. [8,45] The new peroxy radical is highly reactive, it abstracts active hydrogen from the same chain or another PP molecule giving rise to the hydroperoxide species, as well as another PP˙ radical, through which the propagation process continues.

$[\ldots(\text{-}\dot{} O\text{-}O\text{-}C(CH_3)CH_2)(HC(CH_3)CH_2)_{n-1}\text{-}\ldots] + [\ldots\text{-}(HC(CH_3)CH_2)(HC(CH_3)CH_2)_{n-1}\text{-}\ldots] \rightarrow$
$[\ldots(\text{-H-O-O-C-}(CH_3)CH_2)\ (HC(CH_3)CH_2)_{n-1}\text{-}\ldots] + [\ldots\text{-}(\dot{} C(CH_3)\text{-}CH_2)\ (HC(CH_3)CH_2)_{n-1}\text{-}\ldots]$ (iii)
Or $PP\text{-}O\text{-}O\dot{} + \text{H-PP} \rightarrow PP\text{-}O\text{-}O\text{-}H + PP\dot{}$ $\Delta H = +463 - 413 = -50$ kJ/mol, exothermic

Formation of the hydroperoxide in reaction (iii) involves breaking a C-H (413 kJ/mol) bond and formation of O-H bond (463 kJ/mol) therefore, it is exothermic and has a lower activation energy than the previous steps. Conversion of hydroperoxide to oxide and hydroxide (reaction iv), has a barrier of energy around 143 kJ/mol, hence it is not favorable. [56]

$[\ldots\text{-}(\text{-C-O-OH}\ (CH_3)CH_2)\ (HC(CH_3)CH_2)_{n-1}\text{-}\ldots] \rightarrow \ldots(\text{-}\dot{} OC(CH_3)CH_2)(HC(CH_3)CH_2)_{n-1\ldots}] + \dot{} OH$ (iv)
$PP\text{-}O\text{-}O\text{-}H \rightarrow PP\text{-}O\dot{} + \dot{} O\text{-}H$ $\Delta H = +143$ endothermic, not favorable

However, the relatively low activation energy of the thermo-oxidative decomposition of PC-PP (74–145 kJ/mol, **Table 3**, average column) experimentally obtained suggests that instead, reaction (v) with the lower bimolecular decomposition energy barrier (E_a ~ 83 kJ/mol) shall be the limiting step for thermo-oxidative degradation, inter- and intramolecular reactions as:

$PP\text{-}O\text{-}O\text{-}H + PP\text{-}H \rightarrow PP\dot{} + PP\text{-}O\dot{} + \dot{} H\text{-}O\text{-}H$ $\Delta H = 143 + 413 - 463 = +83$ kJ/mole endothermic (v)

Then PP˙ follows the reaction (ii) and the alkoxyl radical, can also effectively abstract hydrogen from the remaining polymers as:

$PP\text{-}O\dot{} + \text{H-PP} \rightarrow PP\text{-}O\text{-}H + \dot{} PP$ $\Delta H = 413 - 463 = -50$ kJ/mol, exothermic

Reaction (v) increases the concentration of the radical species involved in the propagation step (iii & vi), and thereby accelerates oxidative degradation. The overall process turns highly exothermic under excess oxygen (air). As **Fig. *4*** shows, the estimated activation energy is fairly constant, below 90 kJ/mol, during the first 50% of the PC-PP degradation (**Table 3**) and higher than 145 kJ/mol at the higher end, α > 0.9. These results suggest that the kinetic process at lower α values is limited by a single reaction, the peroxide radical decomposition. For the degradation at α > 0.90, the activation energy increases sharply, from 145 to 176 kJ/mol. This amount of E_a was also observed for the initial stages of PP degradation under nitrogen. This suggests that the later stages of thermo-oxidative degradation are likely to occur via the same pathway that involves degradation of PP in an inert atmosphere, initiated by random scission of the residues, which may be a cross-linked of various short chains.

V. Conclusions

The activation energy associated with the thermo-oxidation of PC-PP was determined by the model-free method expressed by **Eq. 6**. The obtained values of $\mathbf{E_a}$ were independent of the specific form of $f(\alpha)$ as was expected from model-free methods. The correlation coefficients of the regressions indicated that the PC-PP pyrolysis leaned towards the tridimensional diffusion process rather than towards the powered models. Knowing that the adequateness of the rate equation to describe the process and the kinetic mechanism of the oxidative decomposition of PC-PP goes far beyond the issue of the goodness of statistical fit observed by the values of r^2.

The value of the intercept, ln**A**, which describes the frequency of vibrations of the activated complex, and directly relates to the entropy of reaction, depending on the form of $f(\alpha)$, as shown in **Table 4 & Fig. *4*(b)**. Therefore, meaningful interpretability of the determined triplets depends on whether the selected rate equation adequately captured the essential features of the process mechanism, not the excellent fits to the data. In this case, the fittings that described the sigmoidal nature of PC-PP thermal oxidation are the most meaningful ones.

Acknowledgments

This work was supported by the National Institute of Food and Agriculture, U.S. Department of Agriculture, Evans-Allen project number SCX-311-21-17 and SCX-311-29-21. Also, we acknowledge the support of Dr. Judy Salley, the Department Chair, and Dr. Louis Whitesides, the Director of 1890-Research programs. Any opinions, findings, conclusions, or recommendations expressed in this material are those of the authors and do not necessarily reflect those of the Funding Agency.

References

[1]. Geyer, R.; Jambeck, J. R.; Law, K. L. Production, use, and fate of all plastics ever made. Sci. Adv. **2017,** 3, 1-5 e1700782. https://doi.org/10.1126/sciadv.1700782

[2]. PP production U.S. 2018. Statista, www.statista.com › Chemicals & Resources › Plastic & Rubbe, Downloaded March 10, 2020.

[3]. https://www.globenewswire.com/news-release/2019/08/01/1895698/0/en/Polypropylene-Market-To-Reach-USD-155-57-Billion-By-2026-Reports-And-Data.html. Aug. 01, 2019 (GLOBE NEWSWIRE) -- Increasing demand for polypropylene from the packaging industry is estimated to stimulate market demand. Downloaded March 10, 2020.

[4]. Das, P.; Tiwari, P.; The effect of slow pyrolysis on the conversion of packaging waste plastics (PE and PP) into fuel. Waste Manag. **2018**, 79, 615-624. https://doi.org/10.1016/j.wasman.2018.08.021

[5]. Ouyang, Y.; Mauri, M.; Pourrahimi, A. M.; Östergren, I.; Lund, A.; Gkourmpis, T.; Prieto, O.; Xu, X.; Hagstrand, P.-O.; Müller, C.; Recyclable polyethylene insulation via reactive compounding with a maleic anhydride-grafted polypropylene. ACS Applied Polymer Materials **2020** 2 (6), 2389-2396 https://doi.org/10.1021/acsapm.0c00320

[6]. Peterson, J. D.; Vyazovkin, S.; Wight, C.A. Kinetics of the thermal and thermo-oxidative degradation of polystyrene, polyethylene and poly(propylene). Macromol. Chem. Phys. **2001**, 202, 775–784. https://doi.org/10.1002/1521-3935(20010301)202:6<775::AID-MACP775>3.0.CO;2-G

[7]. Karimpour- Motlagh, N.; Khonakdar, H. A.; Jafari, S. H.; Panahi- Sarmad, M.; Javadi, A.; Shojaei, S.; Goodarzi, V.; An experimental and theoretical mechanistic analysis of thermal degradation of polypropylene/polylactic acid/clay nanocomposites 2019, 30, 2695-2706 https://doi.org/10.1002/pat.4699

[8]. Speight, J. G.; Monomers, polymers, and plastics in Handbook of Industrial Hydrocarbon Processes, Chapter 10 - Combustion of hydrocarbons. Gulf Professional Publishing, 2nd Ed. **2020**, 421-463, ISBN 9780128099230, https://doi.org/10.1016/B978-0-12-809923-0.00010-2.

[9]. Kim, T.; Choi, J.; Kim, H. J.; Lee, W.; Kim, B. J.; Comparative study of thermal stability, morphology, and performance of all-polymer, fullerene–polymer, and ternary blend solar cells based on the same polymer donor. Macromolecules **2017,** 50, 6861-6871 https://doi.org/10.1021/acs.macromol.7b00834

[10]. Huang, Y.-C.; Liu, W.-S.; Tsao, C.-S.; Wang, L.; Mechanistic insights into the effect of polymer regioregularity on the thermal stability of polymer solar cells. ACS Appl. Mat. & Interfac. **2019,** 11, 40310-40319 https://doi.org/10.1021/acsami.9b12482

[11]. Cordero, T.; Rodríguez-Maroto, J. M.; García, F.; Rodríguez, J. J. Thermal decomposition of wood in oxidizing atmosphere. A kinetic study from non-isothermal TG experiments. Thermochim. Acta. **1991**, 191, 161-178. https://doi.org/10.1016/0040-6031(91)87247-T

[12]. Guindos, P.; Patel, A.; Kolb, T.; Meinlschmidt, P.; Schlüter, F.; Plinke, B. Experimental and numerical characterization of the influence of a smoldering cellulosic substrate on a cigarette's ignition propensity test. Fire Technol. **2018**, 54, 669-688. https://doi.org/10.1007/s10694-017-0699-2

[13]. Orfao, J. J. M.; Antunes, F. J. A.; Figueiredo, J. L.; Pyrolysis kinetics of lignocellulosic materials—three independent reactions model. Fuel **1999**, 78, 349-358. https://doi.org/10.1016/S0016-2361(98)00156-2

[14]. Thipkhunthod, P.; Meeyoo, V.; Rangsunvigit, P.; Kitiyanan, B.; Siemanond, K.; Rirksomboon. T. Pyrolytic characteristics of sewage sludge. Chemosphere, **2006,** 64, 955-962. https://doi.org/10.1016/j.chemosphere.2006.01.002

[15]. Jenekhe, S.A.; Lin, J.W.; Sun, B. Kinetics of the thermal degradation of poly(ethylene terephthalate). Thermochim Acta, **1983**, 61, 287-299. https://doi.org/10.1016/0040-6031(83)80283-4

[16]. Romão, W.; Franco, M. F.; Corilo, Y. E.; Eberlin, M. N.; Spinacé, M. A. S.; De Paoli, M.-A. Poly(ethylene terephthalate) thermo-mechanical and thermo-oxidative degradation mechanisms. Polym. Degrad. Stabil. **2009,** 94, 1849-1859. https://doi.org/10.1016/j.polymdegradstab.2009.05.017

[17]. Cooney, J. D.; Day, M.; Wiles, D. M. Thermal degradation of poly (ethylene terephthalate): a kinetic analysis of thermogravimetric data. J. Appl. Polym. Sci. **1983**, 28, 2887-2902. https://doi.org/10.1002/app.1983.070280918

[18]. Antal, M.J.; Varhegyi, G.; Cellulose pyrolysis kinetics: The current state of knowledge. Ind. Eng. Chem. Res. **1998**, 37, 1267 https://doi.org/10.1021/ie00042a001

[19]. Jakab, E.; Faix, O.; Till, F.; Székely, T.; Thermogravimetry/mass spectrometry study of six lignins within the scope of an international round robin test. J. Anal. Appl. Pyrol. **1995**, 35, 167-179. https://doi.org/10.1016/0165-2370(95)00907-7

[20]. Bilbao, R.; Millera, A.; Arauzo, J.; Thermal decomposition of lignocellulosic materials: influence of the chemical composition. Thermochim. Acta **1989**, 143, 149-159. https://doi.org/10.1016/0040-6031(89)85052-X

[21]. Werner, K; Pommer, L.; Broström, M. Thermal decomposition of hemicelluloses J. Analy. Appl. Pyroly. **2014**, 110, 130-137 https://doi.org/10.1016/j.jaap.2014.08.013

[22]. Bar-Gadda, R.; The kinetics of xylan pyrolysis. Thermochim. Acta **1980**, 42, 153-163. https://doi.org/10.1016/0040-6031(80)87099-7

[23]. Wu, Y.; Dollimore, D. Kinetic studies of thermal degradation of natural cellulosic materials Thermochim. Acta. **1998**, 324, 49-57. https://doi.org/10.1016/S0040-6031(98)00522-X

[24]. Criado, J. M.; Ortega, A.; Gotor, F. Correlation between the shape of controlled-rate thermal analysis curves and the kinetics of solid-state reactions. Thermochim. Acta **1990**, 157, 171−179. https://doi.org/10.1016/0040-6031(90)80018-T

[25]. Ozawa, T. Temperature control modes in thermal analysis. J. Therm. Anal. Calorim. **2001**, 64, 109-126. https://doi.org/10.1023/A:1011580811822

[26]. Ozawa, T. Controlled rate thermogravimetry: New usefulness of controlled rate thermogravimetry revealed by decomposition of polyimide. J. Therm. Anal. Calorim. **2000**, 59, 375-384. https://doi.org/10.1023/a:1010125121227

[27]. Wikipedia https://en.wikipedia.org/wiki/Polypropylene visited Feb 20, 2021

[28]. Brown, M. E.; Maciejewski, M.; Vyazovkin, S.; Nomen, R.; Sempere, J.; Burnham, A.; Opfermann, J.; Strey, R.; Anderson, H. L.; Kemmler, A.; Keuleers, R.; Janssens, J.; Desseyn, H. O.; Li, C.-R.; Tang, T.B.; Roduit, B.; Malek, J.; Mitsuhashi, T. Computational aspects of kinetic analysis. Part A: The ICTAC kinetics project: data, methods, and results. Thermochim. Acta, 2000, 355, 125–143. https://doi.org/10.1016/S0040-6031(00)00443-3

[29]. Sestak, J., Science of heat and thermophysical studies. a generalized approach to thermal analysis. Elsevier, Amsterdam **2005**

[30]. Vyazovkin, S. Recent advances, techniques and applications. The Handbook of thermal analysis and calorimetry. Brown, M.E.; Gallagher, P.K. (Eds.), vol. 5 Elsevier **2008**, p 503.

[31]. Brown, M. E. Introduction to thermal analysis (2nd ed.) Kluwer, Dodrecht **2001**.

[32]. Perejón, A; Sánchez-Jiménez, P. E.; Criado, J. M.; Pérez-Maqueda, L.A. Kinetic analysis of complex solid-state reactions. A new deconvolution procedure. The J. Phys. Chem. B **2011,** 115, 1780-1791. https://doi.org/10.1021/jp110895z

[33]. Georgieva, V.; Vlaev, L.; Gyurova, K. Non-Isothermal Degradation kinetics of $CaCO_3$ from different origin. J. Chem. **2012, 2013**, 2090-9063 https://doi.org/10.1155/2013/872981

[34]. Sohoni, G.B.; Mark, J. E. Thermal stability of in situ filled siloxane elastomers. J. Appl. Polymer Sci. **1992**, 45, 1763-1775. https://doi.org/10.1002/app.1992.070451010

[35]. Abate, L.; Calanna, S.; Pollicino, A.; Recca, A. Thermal stability of a novel poly(ether ether ketone ketone) (PK99). Polym. Eng. Sci. **1996**, 36, 1782-1788. https://doi.org/10.1002/pen.10573

[36]. Rao, M.P.R.; Rao, B.S.M.; Rajan, C.R.; Ghadage, R.S. Thermal degradation kinetics of phenol-crotonaldehyde resins. Polym. Degrad. Stab. **1998**, 61, 283-288. https://doi.org/10.1016/S0141-3910(97)00210-3

[37]. Burnham, A. Computational aspects of kinetic analysis.: Part D: The ICTAC kinetics project -multi-thermal-history model-fitting methods and their relation to isoconversional methods. Thermochim. Acta 355 **2000** 165-170. https://doi.org/10.1016/S0040-6031(00)00446-9

[38]. Bonnet, E.; White, R. L. Species-specific isoconversion effective activation energies derived by thermogravimetry–mass spectrometry. Thermochimica Acta 311 **1998** 81-86. https://doi.org/10.1016/S0040-6031(97)00411-5

[39]. Chien, J. C. W.; Kiang, J. K. Y.; Polymer reaction. 9. Effect of polymer-bound chromium on oxidative pyrolysis of poly(propylene). Macromolecules 1980, 13, 2, 280-288. https://doi.org/10.1021/ma60074a015

[40]. Westerhout, R. W. J.; Balk, R. H. P.; Meijer, R.; Kuipers, J. A. M.; van Swaaij, W. P. M.; Examination and evaluation of the use of screen heaters for the measurement of the high temperature pyrolysis kinetics of polyethene and polypropene. *Ind. Eng. Chem. Res.* 1997, *36*, 3360 https://doi.org/10.1021/ie960502e

[41]. Vyazovkin, S.; Wight, C. A.; Model-free and model-fitting approaches to kinetic analysis of isothermal and nonisothermal data. Thermochim. Acta **1999**, 340/ 341, 53-68. https://doi.org/10.1016/S0040-6031(99)00253-1

[42]. Rabek, J. F. "Oxidative Degradation of Polymers", in: Comprehensive Chemical Kinetics, vol. 14, C. H. Bamford, C. F. H. Tipper, Eds., Elsevier, Amsterdam 1975, p. 425.

[43]. Borden, W. T.; Hoffmann, R.; Stuyver, T.; Chen, B. Dioxygen: What makes this triplet diradical kinetically persistent? J. Am. Chem. Soc. 2017 139, 9010-9018 https://doi.org/10.1021/jacs.7b04232

[44]. Blanksby, S. J.; Ellison, G. B. Bond dissociation energies of organic molecules. Acc. Chem. Res. 2003, 36, 255-263. https://doi.org/10.1021/ar020230d

[45]. Reich, L.; Stivala, S. S. "Elements of Polymer Degradation", McGraw-Hill, New York 1971.